

A synthetic data set for validation of tracer kinetic modelling and model-driven registration in DCE-MRI

G. A. Buonaccorsi¹, G. J. Parker¹

¹Imaging science and Biomedical Engineering, University of Manchester, Manchester, Manchester, United Kingdom

Introduction In clinical quantitative dynamic contrast enhanced MRI (DCE-MRI), it is difficult to verify the accuracy of estimates of kinetic model parameters such as K^{trans} , v_e and v_p , as we do not know the ‘true’ parameter values (ground truth). The problem is exacerbated when we apply motion-correction algorithms in addition to model fitting, as we need to validate both the image registration procedure and the fitting process. Therefore, as an initial step towards a complete validation framework, we have developed a synthetic DCE-MRI data set (software phantom) that incorporates the effects of contrast agent accumulation and washout, translational motion, and noise. Using this phantom and tracer kinetic modelling¹, we show that a recently introduced kinetic model-driven registration algorithm² is able to recover accurate parameter values from motion-corrupted synthetic data.

Synthetic Data The synthetic data comprise a collection of nested cuboids of “pseudo-tissues”, to which we have assigned characteristic values for the parameters of an extended Kety tracer kinetic model (including a v_p term)³, as well as initial values for pseudo-tissue T_1 and S_0 . We used the model along with a high temporal resolution population-averaged arterial input function⁴ to generate a time series of 100 simulated spoiled gradient echo (Fast Field Echo) image volumes with a TR of 4 ms, 30° nominal flip angle, a temporal resolution of 4.03 s and a matrix of $128 \times 128 \times 25$ voxels of size $2.5 \times 2.5 \times 4.0$ mm³. The image and acquisition parameters were chosen to approximate those of a typical DCE-MRI acquisition in our centre. We added motion and noise corruption by applying a sinusoidal translation with a random component only to the “tumour” pseudo-tissues and zero-mean Gaussian noise with a signal-to-noise ratio (SNR) of 10. Fig. 1 shows three example time points from a synthetic dynamic series, showing synthetic “muscle” (background), “fat” (mid-size square), “artery” (small square), and “tumour” (arrows) with an enhancing rim and a non-enhancing core.

Methods We obtained 3D maps of K^{trans} , v_e and v_p from the static and motion-corrupted synthetic data by fitting the extended Kety model in a volume of interest (VOI) encompassing the tumour, using the locally-written MaDyM package. For the motion-corrupted sets, we then performed kinetic model-driven registration and repeated the model fitting.

Results For the static synthetic data, the 3D maps took the expected form of pseudo-tissue regions with uniform intensities corresponding to the input parameter values, corrupted only by noise: see e.g. the K^{trans} map of Fig. 2(a). Fig. 3 compares the simulation input values with the median parameter estimates from pure pseudo-tissue VOIs defined on the static synthetic data (labelled “Static”) – the estimates agree to within the noise level except for the core v_e , which was underestimated due to the slow enhancement and the low signal level.

Adding motion to the synthetic data corrupted the parameter estimates, resulting in the K^{trans} maps of Fig. 2(b) and the median parameter estimates labelled “Pre-reg” in Fig. 3. As expected, most of the distortion in the K^{trans} maps occurred at the borders between the pseudo-tissues, because in these voxels motion mixes the contributions of the pseudo-tissues to the time series data. As the through-plane motion was of greater magnitude (to simulate the greater cranio-caudal motion expected with breathing), the sagittal and coronal views show greater through-plane corruption (arrowed on Fig. 2(b)).

Model-driven registration restored the median parameter estimates to approximately those obtained from the static data (Fig. 3 – labelled “Post-reg”) and significantly reduced corruption in the 3D maps, although residual K^{trans} corruption can be seen in Fig 2(c) as the motion was not perfectly recovered at a sub-voxel level. The significant benefit brought by model-driven registration to the voxel-by-voxel fitting process is clear from the single voxel fitting results of Fig. 4, where the contrast agent concentration time course resulting from the model fit to the post-registration data is a much closer approximation to the true time course than the poor fit obtained from the motion-corrupted raw data.

Discussion Our MaDyM fitting software was able to estimate the kinetic parameters from the static synthetic data with good accuracy. Kinetic model-driven registration was able to restore the parameter estimates from the motion-corrupted synthetic data by correcting for the induced motion, again with good accuracy.

The ability to test DCE-MRI modelling and registration processes against synthetic ground truth brings considerable benefits, as the difficulties in obtaining ground truth from patient or even animal studies are almost certainly insurmountable. The synthetic data set presented herein takes a significant step towards providing that ground truth. While in particular the registration was not a difficult challenge in this simple data set, its simplicity is not a disadvantage, allowing a straightforward interpretation of the results obtained. If greater realism is required, within the framework we have developed we can readily incorporate more detailed kinetic models, and more complex anatomical geometries with more realistic motion patterns.

We propose that synthetic data of this type will prove invaluable for validating DCE-MRI techniques, particularly when they are to be used in clinical trials when standardisation and validation must be performed to exacting standards.

References 1. Jackson A, Buckley DL, Parker GJM (eds.) *Dynamic contrast-enhanced magnetic resonance imaging in oncology*. Springer, Berlin (2005). 2. Buonaccorsi GA *et al Lect Notes Comp Sci*, **3749** 91-98, 2005. 3. Tofts PS *et al. J Magn Reson Imag* **10**, 223-232, 1999. 4. Parker GJM *et al. Proc Int Soc Magn Reson Med*, 2101, 2005.

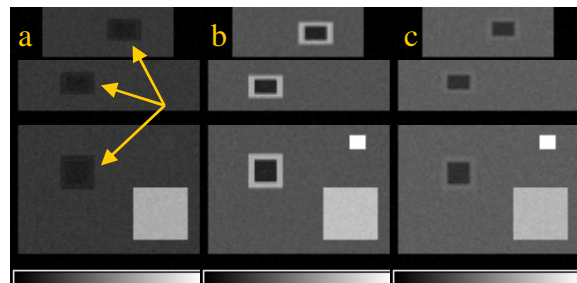


Figure 1. Orthogonal views of the synthetic data at pre-bolus (a), maximum enhancement (b) and post-bolus (c) time points.

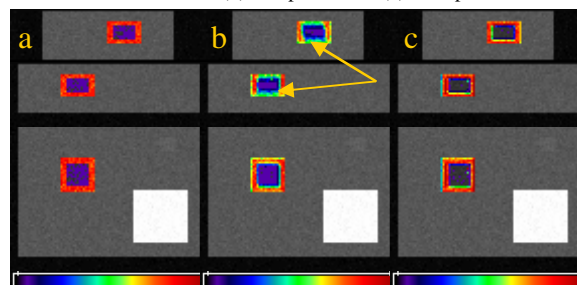


Figure 2. K^{trans} maps from static (a) and moving synthetic data, pre- (b) and post- (c) registration. Scale is from 0 to 0.18 min^{-1} .

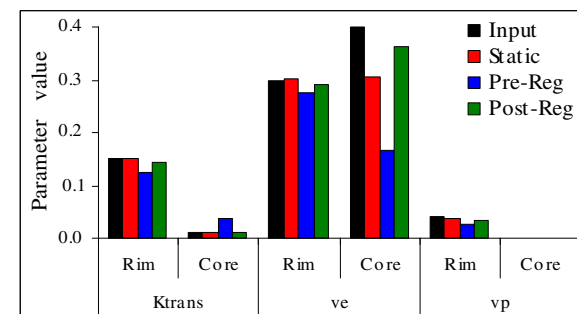


Figure 3. Median model parameter values for pure-tissue VOIs defined on the static and moving synthetic data sets (SNR = 10).

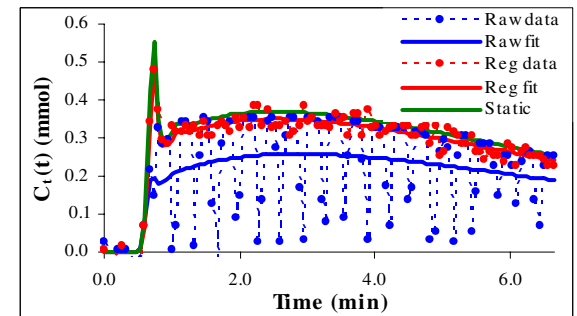


Figure 4. Single voxel model fit results for static synthetic data and moving synthetic data before and after registration.